ARTICLES

Journal of Semiconductors
(2023) 44, 062801
doi: 10.1088/1674-4926/44/6/062801

JOS

Homoepitaxial growth of (100) Si-doped β-Ga_2O_3 films via MOCVD

Wenbo Tang[1, 2], Xueli Han[3, 4], Xiaodong Zhang[1, 2], Botong Li[1, 2], Yongjian Ma[1, 2], Li Zhang[2], Tiwei Chen[1, 2], Xin Zhou[2], Chunxu Bian[2], Yu Hu[1, 2], Duanyang Chen[3], Hongji Qi[3, 4, †], Zhongming Zeng[1, 2], and Baoshun Zhang[1, 2, †]

[1]School of Nano-Tech and Nano-Bionics, University of Science and Technology of China, Hefei 230026, China

[2]Nanofabrication facility, Suzhou Institute of Nano-Tech and Nano-Bionics, Chinese Academy of Sciences, Suzhou 215123, China

[3]Research Center of Laser Crystal, Shanghai Institute of Optics and Fine Mechanics, Chinese Academy of Sciences, Shanghai 201800, China

[4]Hangzhou Institute of Optics and Fine Mechanics, Hangzhou 311421, China

Abstract: Homoepitaxial growth of Si-doped β-Ga_2O_3 films on semi-insulating (100) β-Ga_2O_3 substrates by metalorganic chemical vapor deposition (MOCVD) is studied in this work. By appropriately optimizing the growth conditions, an increasing diffusion length of Ga adatoms is realized, suppressing 3D island growth patterns prevalent in (100) β-Ga_2O_3 films and optimizing the surface morphology with [010] oriented stripe features. The slightly Si-doped β-Ga_2O_3 film shows smooth and flat surface morphology with a root-mean-square roughness of 1.3 nm. Rocking curves of the (400) diffraction peak also demonstrate the high crystal quality of the Si-doped films. According to the capacitance–voltage characteristics, the effective net doping concentrations of the films are 5.41×10^{15} – 1.74×10^{20} cm^{-3}. Hall measurements demonstrate a high electron mobility value of 51 $cm^2/(V{\cdot}s)$, corresponding to a carrier concentration of 7.19×10^{18} cm^{-3} and a high activation efficiency of up to 61.5%. Transmission line model (TLM) measurement shows excellent Ohmic contacts and a low specific contact resistance of 1.29×10^{-4} $\Omega{\cdot}cm^2$ for the Si-doped film, which is comparable to the Si-implanted film with a concentration of 5.0×10^{19} cm^{-3}, confirming the effective Si doing in the MOCVD epitaxy.

Key words: homoepitaxial growth; MOCVD; Si-doping films; high activation efficiency; Ohmic contacts

Citation: W B Tang, X L Han, X D Zhang, B T Li, Y J Ma, L Zhang, T W Chen, X Zhou, C X Bian, Y Hu, D Y Chen, H J Qi, Z M Zeng, and B S Zhang, Homoepitaxial growth of (100) Si-doped β-Ga_2O_3 films via MOCVD[J]. *J. Semicond.*, 2023, 44(6), 062801. https://doi.org/10.1088/1674-4926/44/6/062801

1. Introduction

As an ultrawide bandgap semiconductor material for next-generation high power electronics, β-Ga_2O_3 has attracted enormous attention due to its high breakdown field strength of 8 MV/cm, a large Baliga's figure of merit of 3444, and the availability of high-quality melt-grown native substrates[1–3]. Many β-Ga_2O_3 electronic devices such as Schottky barrier diodes[4–6], MOSFETs[7, 8], FinFETs[9–11], and CAVETs[12, 13] have already been successfully demonstrated, which reveal their great potential in high-power electronics. To further improve their performance, it is essential to obtain epitaxial β-Ga_2O_3 films with high crystal quality. To date, the homoepitaxy of β-Ga_2O_3 films is still confronted with various challenges such as twins and stacking faults, despite the perfect crystalline match between the film and the substrate due to immature research status[14–17]. Various epitaxial growth techniques for β-Ga_2O_3 films have been demonstrated over the past few years, such as halide vapor phase epitaxy (HVPE)[18, 19], molecular beam epitaxy (MBE)[20, 21], low-pressure chemical vapor deposition (LPCVD)[22, 23], metalorganic chemical vapor deposition (MOCVD)[24–26], and carbothermal reduction rapid growth method[27]. With the available (100), (010), (001), and ($\bar{2}$01) orientated substrates[28], the homoepitaxy of β-Ga_2O_3 films exhibits a great development prospect. Owing to the anisotropic characteristics, the crystal orientation of β-Ga_2O_3 substrates has an enormous impact on the quality of the epilayers. Among them, (100) oriented substrates can be easily prepared, but its epitaxy is still challenging due to the preferred cleavage plane with the lowest surface energy[29]. 2D island growth mode usually plays a dominant role due to the limited diffusion length of the (100) surface adatoms[30], which causes deterioration of the crystal quality. Many efforts have been made on the homoepitaxial growth of (100) β-Ga_2O_3 thin films[20, 31, 32]. In addition, the high concentration n-type doping in β-Ga_2O_3 still remains challenging, and Si-ion implantation is usually used in the Ohmic contact region nowadays[33–35]. Therefore, the homoepitaxial growth of (100) Si-doped β-Ga_2O_3 thin films with high concentration is important for β-Ga_2O_3 devices.

In this work, (100) β-Ga_2O_3 films with Si-doping were grown on semi-insulating (100) substrates by MOCVD, which is a preferred growth method for semiconductor device technologies at the industrial level. The suppression of the 2D island growth mode was demonstrated through the optimization of the growth conditions, such as VI/III ratio, temperature and chamber pressure. A promotion of the surface mor-

Correspondence to: H J Qi, qhj@siom.ac.cn; B S Zhang, bszhang2006@sinano.ac.cn

Received 29 DECEMBER 2022; Revised 21 JANUARY 2023.

©2023 Chinese Institute of Electronics

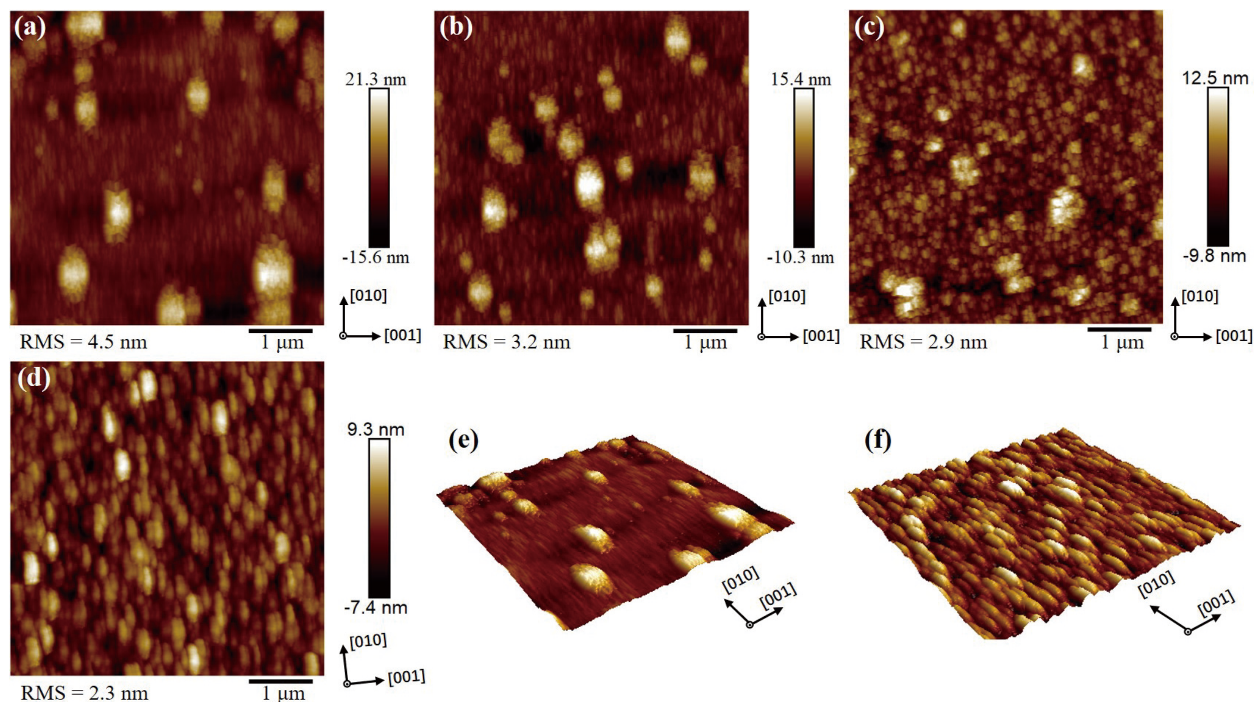

Fig. 1. (Color online) Surface morphologies of β-Ga_2O_3 films grown in different conditions. AFM topography images of sample (a) A_1, (b) A_2, (c) A_3 and (d) A_4. 3D AFM images of sample (e) A_1 and (f) A_4.

phology of the epitaxial films from Si doping were confirmed, which proved the facilitation of the growth kinetics. The obtained (100) β-Ga_2O_3 films exhibited a smooth surface with high crystal quality, even for the heavy doped films. Excellent Ohmic contacts and high current density were achieved.

2. Experiments

The (100) β-Ga_2O_3 epitaxial films were grown via MOCVD on semi-insulating β-Ga_2O_3 substrates with no intentional offcut produced by Hangzhou Fujia Gallium Technology Co., Ltd. Before the epi-growth, the substrates were immersed in piranha solution and then hydrofluoric acid to remove the possible Si contaminants on the substrate surface and followed with in-situ annealing for 15 min at 800 °C under an O_2 atmosphere. Triethylgallium (TEGa), high-purity oxygen gas (O_2), and silane (SiH_4) were used as Ga and O precursors and Si dopants, respectively. High-purity nitrogen (N_2) was used as the carrier gas. The growth temperature was set at 800–900 °C with the pressure kept at 10 kPa. The growth rates of the epitaxial films were in the range of 4–7 nm/min. Atomic force microscopy (AFM), high-resolution X-ray diffraction (HRXRD), scanning electron microscopy (SEM), time-of-flight secondary ion mass spectroscopy (ToF-SIMS), and Hall measurement were applied to characterize the material properties of the (100) β-Ga_2O_3 films. A Keysight B1505A Power Device Analyzer was used to measure the electrical characteristics of the devices based on the epi-films.

3. Results and discussion

Compared to (010) and (001) β-Ga_2O_3, the homoepitaxy of (100) β-Ga_2O_3 films is up against more issues owing to the low surface energy and the facile cleavage plane[36]. Slow growth rate[28] and 2D island growth mode[37] are commonly seen in the (100) β-Ga_2O_3 films growth process. As the absorption and diffusion length of Ga adatoms on the (100) surface define low incorporation efficiency, random nucleation and island formation will easily occur. And the lack of energetically favorable lattice sites induces more formation of 3D islands by the encounter of Ga adatoms[30], resulting in the roughening of the surface. To improve the surface morphology and get a smooth film, suppressing the formation of 3D islands is essential. Usually, an O-rich regime is adopted in the growth environment, and the decrease of the O/Ga ratio can bring an increasing diffusion length of Ga adatoms[31]. In the experiments, the TEGa molar flow rate was 68.2 μmol/min. The β-Ga_2O_3 films grown in different conditions with unintentional doping were labeled as sample A_1, A_2, A_3 and A_4, respectively. Fig. 1(a) shows the AFM image of sample A_1 grown at 10 kPa and 850 °C with the O/Ga ratio of 1308, showing a root-mean-square (RMS) roughness of 4.5 nm in a 5 × 5 μm^2 scanning area. Scattered islands on the surface contribute to the large roughness and deteriorate the crystal quality. Similar morphology was reported in Ref. [36]. In addition, the islands, 0.3–1.5 μm long and 0.2–0.7 μm wide, with a height of no more than 27 nm, show a fixed orientation along the [010] direction, which is consistent with the stripes in the region without islands. The aligned islands also indicate strong anisotropic characteristics in growth. To suppress the formation of islands, a slightly smaller O/Ga ratio of 1250 was implemented. As can be seen from Fig. 1(b), islands get smaller with an increasing diffusion length of Ga adatoms, accompanied by a smaller RMS roughness of 3.2 nm. To further eliminate the islands, the growth temperature was decreased from 850 to 800 °C. It is found that the big islands disappear and small grains appear instead. The grains have the same arrangement oriented along the [010] direction and some of them even stack as hills. As exhibited in Fig. 1(c), the film surface was filled with aligned grains and had a smaller RMS roughness of 2.9 nm. As the pressure drops to 8 kPa, the length of the grains extends along the [010] direction with

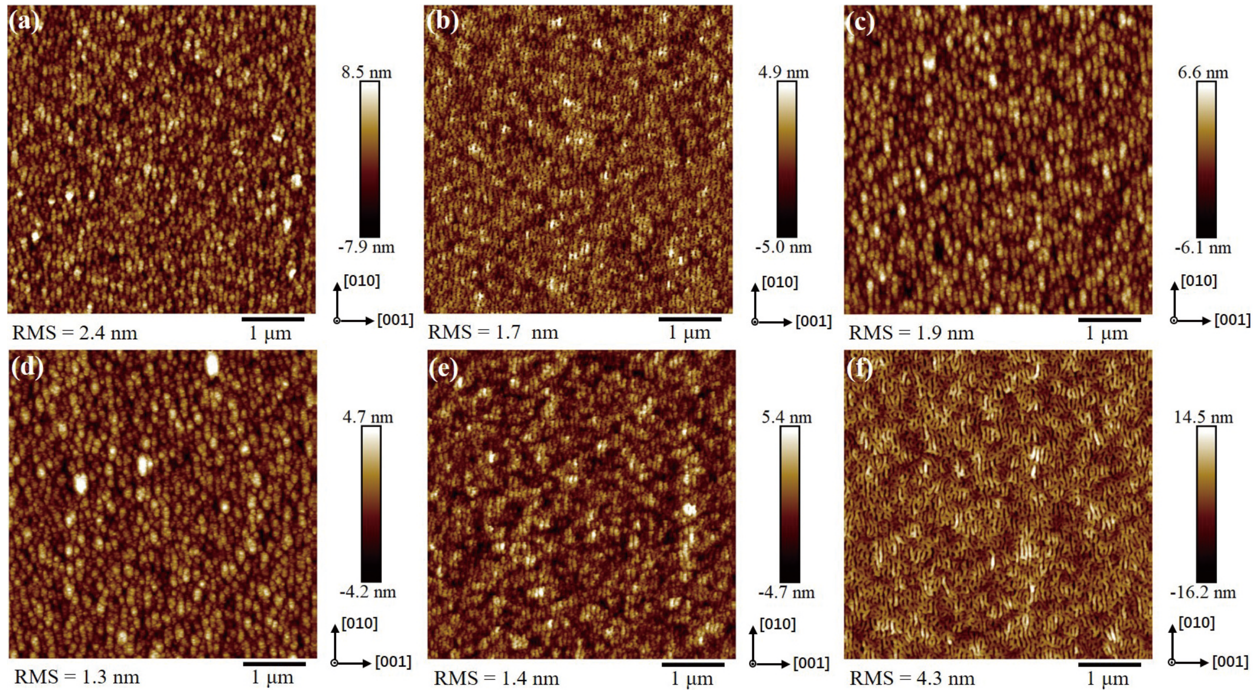

Fig. 2. (Color online) AFM images of the Si-doped β-Ga_2O_3 films grown with different flow rate of SiH_4. (a) B_2, 0.5 sccm. (b) B_3, 1.2 sccm. (c) B_4, 3 sccm. (d) B_5, 6 sccm. (e) B_6, 10 sccm. (f) B_7, 20 sccm.

granular features, which implies that lateral growth along the [010] direction gets stronger. The granular surface morphology is shown in Fig. 1(d), with a length of ~500 nm, a width of ~120 nm, and a height of ~6 nm. The transition from island morphology to granular morphology attributes to the relatively low RMS roughness of 2.3 nm. Figs. 1(e) and 1(f) are the 3D AFM images corresponding to Figs. 1(a) and 1(d), respectively. It can be intuitively seen that oriented 3D islands disperse on the film surface in Fig. 1(e) and oriented granules align on the film surface in Fig. 1(f). The feature of the [010] orientation confirms the anisotropic growth of β-Ga_2O_3. Similar morphology was also reported in the homoepitaxy of ($\bar{2}$01) β-Ga_2O_3 films[38, 39].

Subsequently, the homoepitaxial growth of (100) β-Ga_2O_3 films with different Si-doping concentration was investigated. The samples are labeled as B_1, B_2, B_3, B_4, B_5, B_6 and B_7, with the flow rate of SiH_4 in the growth of 0, 0.5, 1.2, 3, 6, 10, and 20 sccm, respectively. The growth rate of the films was almost unchanged with the introduction of SiH_4. Fig. 2 shows the surface morphologies of the films. Sample B_1 is undoped and has a similar surface morphology to sample A_4, therefore its AFM image is not shown here. It can be seen that the introduction of Si atoms brings a decrease of RMS roughness to the epitaxial films. With 0.5 sccm SiH_4 flow rate, the morphology transforms from granules into narrow and continuous stripes with a width of ~80 nm, as shown in Fig. 2(a). The RMS roughness of sample B_2 is 2.4 nm and stays almost unchanged. Thinner continuous stripes with a width of ~60 nm were found for sample B_3, the films grown with 1.2 sccm SiH_4, resulting in a decreased RMS roughness of 1.7 nm, shown in Fig. 2(b). By gradually further increasing the flow rate of SiH_4, similar morphologies with oriented stripes appeared on the film surface. Figs. 2(c)–2(e) display the surface morphologies of sample B_4, B_5, and B_6, whose RMS roughness is 1.9, 1.3, and 1.4 nm, respectively. The incorporation of Si atoms can suppress random nucleation and island formation during (100) β-Ga_2O_3 growth to a certain extent through the preferred bonding species of Si adatoms to the O atoms, where a similar mechanism was reported in the $(Al_xGa_{1-x})_2O_3$ growth[30]. As a result, a smooth and flat surface was obtained through light Si doping. The coalescence of the original 2D islands was promoted by the distributed Si nucleation sites on the growth surface, facilitating the step-flow growth mode[16]. However, when the doping amount exceeds a certain degree, such as 20 sccm SiH_4, the stripes start to lose their orientation and reveal an undulating surface with increasing RMS roughness. Fig. 2(f) depicts the surface morphology of sample B_7, which has curly stripes and an RMS roughness of 4.3 nm. The weak anisotropic growth may contribute to the above morphology change.

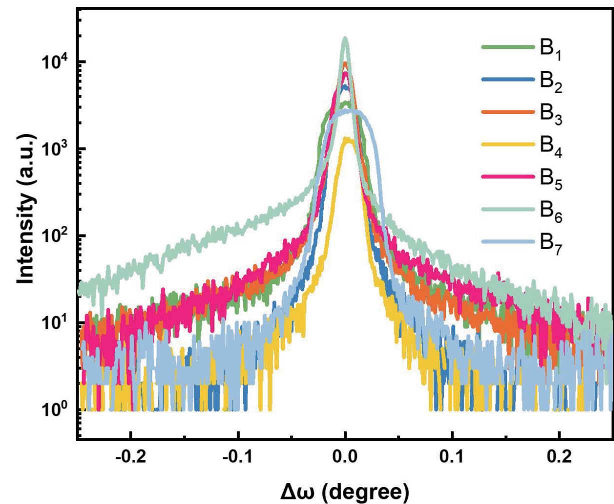

Fig. 3. (Color online) The HRXRD rocking curves of the (400) diffraction peak for the homoepitaxial films.

The effect of Si incorporation on the crystal quality of the epitaxial films was studied through HRXRD. Rocking curves of the (400) diffraction peak of β-Ga_2O_3 were shown in Fig. 3. All

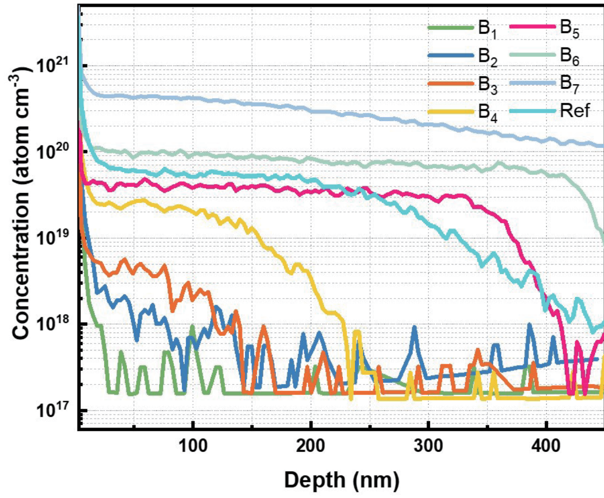

Fig. 4. (Color online) ToF-SIMS profiles of Si for the epitaxial films.

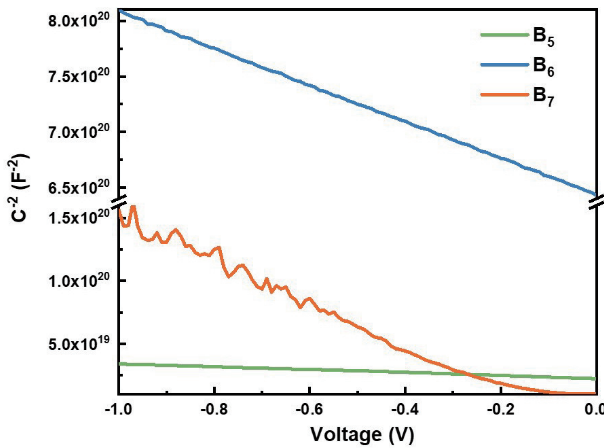

Fig. 5. (Color online) Plot of $1/C^2$–V for the epitaxial β-Ga_2O_3 films with high doping levels.

the films show good crystal quality with the full-width at high maximum (FWHM) of the (400) peak below 60 arcsec, except for the highly doped sample B_7, whose SiH_4 flow rate is 20 sccm. It should be noted that all the prepared films have a thickness of ~400 nm, most of the diffraction signal may come from the substrate as a result. However, if the Si doping leads to a deterioration in crystal quality, a large FWHM should be present, such as for sample B_7, which has a FWHM of 119 arcsec. This suggests new defects are generated in the epitaxial films, and the excess incorporation of Si atoms deteriorates the crystal quality of the β-Ga_2O_3 films. Therefore, to ensure the high crystal quality of the film, the flow rate of SiH_4 in the growth should not exceed 20 sccm.

ToF-SIMS was applied to identify the concentration of Si atoms in the grown β-Ga_2O_3 films. As depicted in Fig. 4, the concentrations of Si atoms of all the films are in the range of 1.57×10^{17} – 2.83×10^{20} cm^{-3}. Note that the detection limit of Si is 1.57×10^{17} cm^{-3}, and a Si-ion implanted film with a concentration of 5.0×10^{19} cm^{-3} is used as the standard sample. For sample B_4, B_5, B_6 and B_7, their Si concentrations are 2.63×10^{19}, 3.46×10^{19}, 7.73×10^{19}, and 2.83×10^{20} cm^{-3}, respectively. Such high doping levels with high crystal quality could be achieved only by Si-ion implantation previously[8, 13, 35, 40–42]. While ion implantation usually results in large lattice damage and requires high-temperature activation[40], which may cause adverse effects on the subsequent process[43, 44]. As a result, the technical route of Si doping in the process of epitaxy can bring more convenience and solutions to semiconductor processing technology.

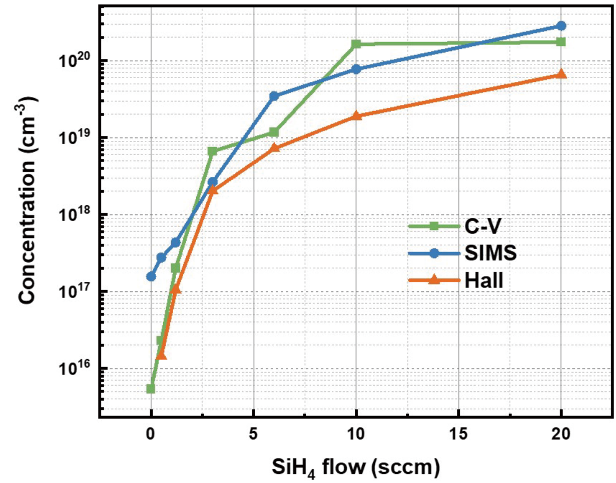

Fig. 6. (Color online) Comparison of the concentrations extracted from C–V, SIMS, and Hall measurements.

A Ti (50 nm)/Au (100 nm) contact was deposited on the film surface as the Ohmic electrode, followed by 475 °C annealing in N_2 atmosphere for 1 min. And a Ni (50 nm)/Au (100 nm) contact was deposited as the Schottky electrode subsequently. Capacitance–voltage (C–V) characteristics of the epitaxial β-Ga_2O_3 films were measured, and the effective net doping concentration (N_D–N_A) can be extracted from the slope of the $1/C^2$–V plots in Fig. 5. The equation is given as

$$\left(\frac{1}{C}\right)^2 = \frac{2\left(V_{bi} + V_R\right)}{e\varepsilon_s\left(N_D - N_A\right)}, \quad (1)$$

where C is the capacitance per unit area, e is the electron charge, V_{bi} is the built-in potential difference, V_R is the applied voltage, and ε_s is the dielectric constant of β-Ga_2O_3. The values of N_D–N_A of the prepared films are 5.41×10^{15}, 2.30×10^{16}, 2.01×10^{17}, 6.65×10^{18}, 1.17×10^{19}, 1.64×10^{20}, and 1.74×10^{20} cm^{-3}, corresponding to the samples B_1, B_2, B_3, B_4, B_5, B_6 and B_7, respectively. The $1/C^2$–V plots of the lightly doped films are not shown here. The small changes of the N_D–N_A between the films grown with 10 and 20 sccm SiH_4 further confirm the excessive Si-doping in B_7. Hall measurement was also used to acquire the effective carrier concentration of the epitaxial films. A high electron mobility value of 51 cm^2/(V·s) at room temperature was achieved for sample B_5 with a carrier concentration of 7.19×10^{18} cm^{-3}. And a high activation efficiency of about 61.5% is obtained for sample B_5 meanwhile. Fig. 6 compares the concentrations extracted from C–V, SIMS, and Hall measurements. The extracted curves have a similar trend, which means the efficiency of Si incorporation gets smaller when the SiH_4 flow rate increases.

Current density–voltage (J–V) characteristics of the epitaxial β-Ga_2O_3 films were measured. Fig. 7(a) shows the J–V characteristics acquired on transmission line model (TLM)[45] patterns of the epitaxial β-Ga_2O_3 films with different Si-doping concentrations in a linear plot. It is clear that the grown films with high doping exhibit good Ohmic contacts. With the proper increase of the flow rate, the resistivity of the film decreases, and B_6 gets the minimum. The significant increase

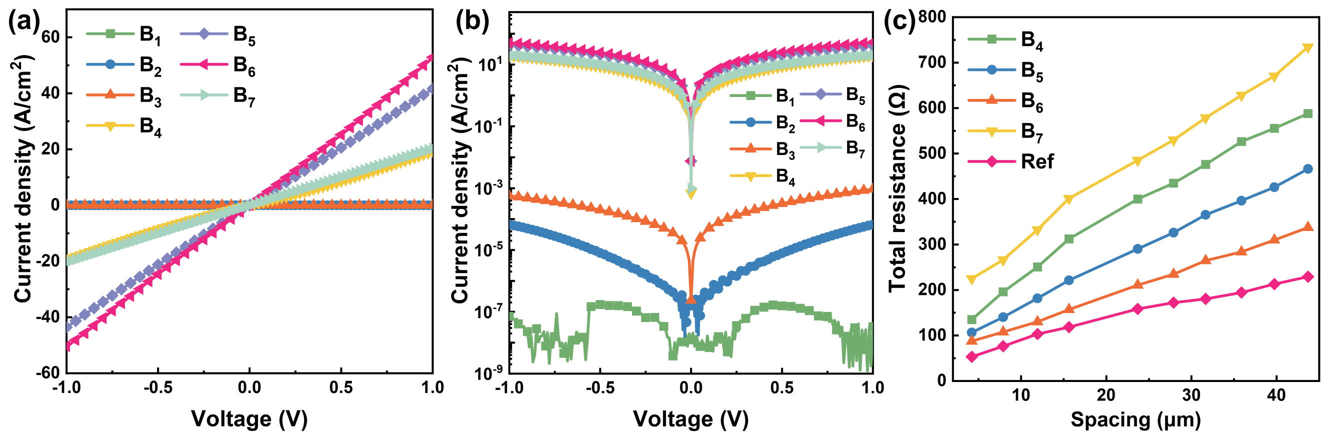

Fig. 7. (Color online) *J*–*V* characteristics of the *β*-Ga_2O_3 films acquired on TLM patterns in (a) a linear plot and (b) a semi-log plot. (c) Linear fit of total resistance as a function of pad spacing.

Table 1. Summary of the electronic characteristics extracted from the TLM measurements corresponding to different contact lengths on the basis of linear TLM theory.

Sample number	R_c (Ω·mm)	R_{SH} (Ω/□)	L_T (μm)	ρ_c (10^{-4} Ω·cm²)
B_4	7.67	2466.93	3.11	2.38
B_5	6.90	1324.57	5.21	3.59
B_6	3.73	1084.55	3.44	1.29
B_7	11.18	1929.83	5.79	6.48
Ref	2.81	751.48	3.74	1.05

in resistivity of B_7 compared to B_5 is due to the deteriorating film quality caused by excessive doping. Fig. 7(b) shows the *J*–*V* characteristics of the epitaxial *β*-Ga_2O_3 films in a semi-log plot. The current density of the high Si-doped film is greater than 10 A/cm². The relationship between the total resistance (R_T) and the pad spacing determined from the *J*–*V* curves of samples with different Si doping amounts is shown in Fig. 7(c), and the data were fitted linearly. Based on the TLM measurements, the contact resistivities, the sheet resistances, the transfer lengths, and the specific contact resistances are extracted, as presented in Table 1. From the fits, the R_c = 3.73 Ω, L_T = 3.44 *μ*m and R_{SH} = 1084.55 Ω/□ of sample B_6 were extracted. The specific contact resistance ρ_c = 1.29 × 10^{-4} Ω·cm² is obtained by this analysis. These excellent electrical conductivities are comparable to the sample Ref in the table, which is the Si-implanted film with a concentration of 5.0 × 10^{19} cm^{-3}, confirming the effective Si doping in the MOCVD epitaxy. The low specific contact resistance and high current density indicate that apart from ion implantation, Si-doped epitaxy can also achieve excellent Ohmic contacts.

4. Conclusion

Homoepitaxial growth of (100) *β*-Ga_2O_3 films and Si doping with different concentration through MOCVD were studied in this work. By adjusting the Ⅵ/Ⅲ ratio, chamber temperature and pressure, the diffusion length of Ga adsorption atoms was increased, inhibiting the 2D island growth mode and resulting in smooth surface morphology. The gradient Si-doping films indicate that the introduction of Si atoms facilitates the growth kinetics and promotes the coalescence of original 2D islands, which is beneficial to the formation of a smooth surface. Apart from the over-doped sample, most of the epitaxial *β*-Ga_2O_3 films with Si-doping exhibit good crystal quality, with (400) FWHM less than 60 arc sec. Based on the *C*–*V* characteristics, an effective net doping concentration from 5.41 × 10^{15} to 1.74 × 10^{20} cm^{-3} was realized. And a high Hall mobility of 51 cm²/(V·s) was also achieved for the sample with a carrier concentration of 7.19 × 10^{18} cm^{-3} and a high activation efficiency of about 61.5%. The epitaxial film demonstrates a low specific contact resistance of 1.29 × 10^{-4} Ω·cm², which is comparable to the Si-implanted film, indicating the effective Si doping in the MOCVD epitaxy. It proves that Si doping in the MOCVD epitaxy of *β*-Ga_2O_3 films can meet the demand of both a high concentration doping and high crystal quality, which provides a solution for the future development of *β*-Ga_2O_3 power devices apart from Si-ion implantation.

Acknowledgements

This work was supported in part by the National Basic Research Program of China (Grant No. 2021YFB3600202), Key Laboratory Construction Project of Nanchang (Grant No. 2020-NCZDSY-008), Jiangxi Province Double Thousand Plan (Grant No. S2019CQKJ2638), Suzhou Science and Technology Foundation (Grant No. SYG202027). The authors would like to thank Nano Fabrication Facility and Vacuum Interconnected Nanotech Workstation (NANO-X) of Suzhou Institute of Nano-Tech and Nano-Bionics, Chinese Academy of Sciences for their technical support. And thank Hangzhou Fujia Gallium Technology Co., Ltd. for its help in crystal growth.

References

[1] Wagner G, Baldini M, Gogova D, et al. Homoepitaxial growth of β-Ga_2O_3 layers by metal-organic vapor phase epitaxy. Phys Status Solidi A, 2014, 211, 27
[2] Higashiwaki M, Sasaki K, Kuramata A, et al. Development of gallium oxide power devices. Phys Status Solidi A, 2014, 211, 21
[3] Rafique S, Karim M R, Johnson J M, et al. LPCVD homoepitaxy of Si doped β-Ga_2O_3 thin films on (010) and (001) substrates. Appl Phys Lett, 2018, 112, 052104
[4] Tang W B, Zhang X D, He T, et al. Temperature-dependent electrical characteristics of β-Ga_2O_3 trench Schottky barrier diodes via self-reactive etching. J Phys D, 2021, 54, 425104
[5] He Q M, Hao W B, Zhou X Z, et al. Over 1 GW/cm² vertical Ga_2O_3 Schottky barrier diodes without edge termination. IEEE Electron

Device Lett, 2022, 43, 264
[6] Lin C H, Yuda Y, Wong M H, et al. Vertical Ga_2O_3 Schottky barrier diodes with guard ring formed by nitrogen-ion implantation. IEEE Electron Device Lett, 2019, 40, 1487
[7] Wang Y B, Xu W H, Han G Q, et al. Channel properties of Ga_2O_3-on-SiC MOSFETs. IEEE Trans Electron Devices, 2021, 68, 1185
[8] Zeng K, Soman R, Bian Z L, et al. Vertical Ga_2O_3 MOSFET with magnesium diffused current blocking layer. IEEE Electron Device Lett, 2022, 43, 1527
[9] Huang H C, Ren Z J, Anhar Uddin Bhuiyan A F M, et al. β-Ga_2O_3 FinFETs with ultra-low hysteresis by plasma-free metal-assisted chemical etching. Appl Phys Lett, 2022, 121, 052102
[10] Hu Z Y, Nomoto K, Li W S, et al. 1.6 kV vertical Ga_2O_3 FinFETs with source-connected field plates and normally-off operation. 2019 31st International Symposium on Power Semiconductor Devices and ICs (ISPSD), 2019, 483
[11] Fabris E, De Santi C, Caria A, et al. Trapping and detrapping mechanisms in β-Ga_2O_3 vertical FinFETs investigated by electro-optical measurements. IEEE Trans Electron Devices, 2020, 67, 3954
[12] Wong M H, Murakami H, Kumagai Y, et al. Aperture-limited conduction and its possible mechanism in ion-implanted current aperture vertical β-Ga_2O_3 MOSFETs. Appl Phys Lett, 2021, 118, 012102
[13] Wong M H, Murakami H, Kumagai Y, et al. Enhancement-mode β-Ga_2O_3 current aperture vertical MOSFETs with N-ion-implanted blocker. IEEE Electron Device Lett, 2020, 41, 296
[14] Sdoeung S, Sasaki K, Kawasaki K, et al. Line-shaped defects: Origin of leakage current in halide vapor-phase epitaxial (001) β-Ga_2O_3 Schottky barrier diodes. Appl Phys Lett, 2022, 120, 122107
[15] Sdoeung S, Sasaki K, Kawasaki K, et al. Probe-induced surface defects: Origin of leakage current in halide vapor-phase epitaxial (001) β-Ga_2O_3 Schottky barrier diodes. Appl Phys Lett, 2022, 120, 092101
[16] Huang H L, Chae C, Hwang J. Perspective on atomic scale investigation of point and extended defects in gallium oxide. J Appl Phys, 2022, 131, 190901
[17] Tadjer M J, Lyons J L, Nepal N, et al. Review—Theory and characterization of doping and defects in β-Ga_2O_3. ECS J Solid State Sci Technol, 2019, 8, Q3187
[18] Nishinaka H, Nagaoka T, Kajita Y, et al. Rapid homoepitaxial growth of (010) β-Ga_2O_3 thin films via mist chemical vapor deposition. Mater Sci Semicond Process, 2021, 128, 105732
[19] Goto K, Murakami H, Kuramata A, et al. Effect of substrate orientation on homoepitaxial growth of β-Ga_2O_3 by halide vapor phase epitaxy. Appl Phys Lett, 2022, 120, 102102
[20] Mazzolini P, Falkenstein A, Galazka Z, et al. Offcut-related step-flow and growth rate enhancement during (100) β-Ga_2O_3 homoepitaxy by metal-exchange catalyzed molecular beam epitaxy (MEXCAT-MBE). Appl Phys Lett, 2020, 117, 222105
[21] Mazzolini P, Bierwagen O. Towards smooth (010) β-Ga_2O_3 films homoepitaxially grown by plasma assisted molecular beam epitaxy: The impact of substrate offcut and metal-to-oxygen flux ratio. J Phys D, 2020, 53, 354003
[22] Zhang Y X, Feng Z X, Karim M R, et al. High-temperature low-pressure chemical vapor deposition of β-Ga_2O_3. J Vac Sci Technol A, 2020, 38, 050806
[23] Ranga P, Bhattacharyya A, Whittaker-Brooks L, et al. N-type doping of low-pressure chemical vapor deposition grown β-Ga_2O_3 thin films using solid-source germanium. J Vac Sci Technol A, 2021, 39, 030404
[24] Chou T S, Bin Anooz S, Grüneberg R, et al. Si doping mechanism in MOVPE-grown (100) β-Ga_2O_3 films. Appl Phys Lett, 2022, 121, 032103
[25] Ikenaga K, Tanaka N, Nishimura T, et al. Effect of high temperature homoepitaxial growth of β-Ga_2O_3 by hot-wall metalorganic vapor phase epitaxy. J Cryst Growth, 2022, 582, 126520
[26] Tang W B, Ma Y J, Zhang X D, et al. High-quality (001) β-Ga_2O_3 homoepitaxial growth by metalorganic chemical vapor deposition enabled by *in situ* indium surfactant. Appl Phys Lett, 2022, 120, 212103
[27] Zhang W H, Zhang H Z, Zhang Z Z, et al. Heteroepitaxial β-Ga_2O_3 thick films on sapphire substrate by carbothermal reduction rapid growth method. Semicond Sci Technol, 2022, 37, 085014
[28] Mazzolini P, Falkenstein A, Wouters C, et al. Substrate-orientation dependence of β-Ga_2O_3 (100), (010), (001), and ($\bar{2}01$) homoepitaxy by indium-mediated metal-exchange catalyzed molecular beam epitaxy (MEXCAT-MBE). APL Mater, 2020, 8, 011107
[29] Mu S, Wang M G, Peelaers H, et al. First-principles surface energies for monoclinic Ga_2O_3 and Al_2O_3 and consequences for cracking of $(Al_xGa_{1-x})_2O_3$. APL Mater, 2020, 8, 091105
[30] Anhar Uddin Bhuiyan A F M, Feng Z X, Johnson J M, et al. MOCVD epitaxy of ultrawide bandgap β-$(Al_xGa_{1-x})_2O_3$ with high-Al composition on (100) β-Ga_2O_3 substrates. Cryst Growth Des, 2020, 20, 6722
[31] Bin Anooz S, Grüneberg R, Wouters C, et al. Step flow growth of β-Ga_2O_3 thin films on vicinal (100) β-Ga_2O_3 substrates grown by MOVPE. Appl Phys Lett, 2020, 116, 182106
[32] Schewski R, Lion K, Fiedler A, et al. Step-flow growth in homoepitaxy of β-Ga_2O_3 (100)—The influence of the miscut direction and faceting. APL Mater, 2018, 7, 022515
[33] Wang C L, Zhou H, Zhang J C, et al. Hysteresis-free and μs-switching of D/E-modes Ga_2O_3 hetero-junction FETs with the $BV^2/R_{on, sp}$ of 0.74/0.28 GW/cm^2. Appl Phys Lett, 2022, 120, 112101
[34] Wang C L, Zhang J C, Xu S R, et al. Progress in state-of-the-art technologies of Ga_2O_3 devices. J Phys D:Appl Phys, 2021, 54, 243001
[35] Sasaki K, Higashiwaki M, Kuramata A, et al. Si-ion implantation doping in β-Ga_2O_3 and its application to fabrication of low-resistance ohmic contacts. Appl Phys Express, 2013, 6, 086502
[36] Oshima T, Arai N, Suzuki N, et al. Surface morphology of homoepitaxial β-Ga_2O_3 thin films grown by molecular beam epitaxy. Thin Solid Films, 2008, 516, 5768
[37] Meng L Y, Bhuiyan A F M A U, Feng Z X, et al. Metalorganic chemical vapor deposition of (100) β-Ga_2O_3 on on-axis Ga_2O_3 substrates. J Vac Sci Technol A, 2022, 40, 062706
[38] Ngo T S, Le D D, Lee J, et al. Investigation of defect structure in homoepitaxial ($\bar{2}01$) β-Ga_2O_3 layers prepared by plasma-assisted molecular beam epitaxy. J Alloys Compd, 2020, 834, 155027
[39] Bhuiyan A F M A U, Feng Z X, Johnson J M, et al. MOCVD growth of β-phase $(Al_xGa_{1-x})_2O_3$ on ($\bar{2}01$) β-Ga_2O_3 substrates. Appl Phys Lett, 2020, 117, 142107
[40] Ma P P, Zheng J, Zhang Y B, et al. Investigation on n-type ($\bar{2}01$) β-Ga_2O_3 ohmic contact via Si ion implantation. Tsinghua Sci Technol, 2023, 28, 150
[41] Nikolskaya A, Okulich E, Korolev D, et al. Ion implantation in β-Ga_2O_3: Physics and technology. J Vac Sci Technol A, 2021, 39, 030802
[42] Lee M H, Chou T S, Bin Anooz S, et al. Exploiting the nanostructural anisotropy of β-Ga_2O_3 to demonstrate giant improvement in titanium/gold ohmic contacts. ACS Nano, 2022, 16, 11988
[43] Sharma R, Law M E, Ren F, et al. Diffusion of dopants and impurities in β-Ga_2O_3. J Vac Sci Technol A, 2021, 39, 060801
[44] Zhang Y N, Zhang J C, Feng Z Q, et al. Impact of implanted edge termination on vertical β-Ga_2O_3 Schottky barrier diodes under OFF-state stressing. IEEE Trans Electron Devices, 2020, 67, 3948
[45] Ranga P, Bhattacharyya A, Chmielewski A, et al. Growth and characterization of metalorganic vapor-phase epitaxy-grown β-$(Al_xGa_{1-x})_2O_3$/β-Ga_2O_3 heterostructure channels. Appl Phys Express, 2021, 14, 025501

Wenbo Tang is a PhD student at University of Science and Technology of China and Suzhou Institute of Nano-Tech and Nano-Bionics of Chinese Academy of Sciences under the supervision of Prof. Baoshun Zhang. His research focuses on the homoepitaxy and power electronics of β-Ga_2O_3.

Hongji Qi received his BS degree from Zhengzhou University in 2000 and his PhD degree from Shanghai Institute of Optics and Fine Mechanics, Chinese Academy of Sciences in 2005. After that, he stayed at the institute as an assistant researcher and became a full researcher in 2011. His research interests include nonlinear crystal materials, novel semiconductor materials and scintillation crystal materials.

Baoshun Zhang received his BS degree from Changchun University of Science and Technology in 1994 and PhD degree from the Institute of Semiconductors, Chinese Academy of Sciences in 2003. Then he joined in Hong Kong University of Science and Technology. Currently, he is a researcher at Suzhou Institute of Nano-Tech and Nano-Bionics, Chinese Academy of Sciences, and his research interests include semiconductor material growth and device technology research.